MODEL-BASED COMPENSATION OF TISSUE DEFORMATION DURING DATA ACQUISITION FOR INTERPOLATIVE ULTRASOUND SIMULATION

Barbara Flach, Maxim Makhinya, and Orcun Goksel

Computer-assisted Applications in Medicine, Computer Vision Lab, ETH Zurich, Switzerland

ABSTRACT

Interpretation of ultrasound relies heavily on the skill and expertise of the performing physician. Therefore, its training is essential, for which computerized virtual-reality simulators can offer a viable solution. In image-based interpolative simulation, a previously acquired 3D ultrasound volume in an undeformed state of the anatomy being interacted is utilized. Acquisition of such volumes involve pressure on the skin by the transducer, thereby the volumes cannot be used directly for simulation. In this work, we propose to correct for tissue deformation caused by the probe during acquisition using volumetric finite-element models locally around the contact area. We show that a generic homogeneous model is sufficient for visual fidelity and for further 3D panorama reconstruction from multiple pressure-compensated volumes. We further show that applying such deformation correction on pre-scan-converted data preserves ultrasound texture more realistically than post-scan-converted data, with respective worst-case losses of 35% vs. 1% intensity standard-deviation.

Index Terms— Interpolative ultrasound simulation, probe pressure, large field-of-view 3D reconstruction.

1. INTRODUCTION

Ultrasound is a widely-used imaging modality in medicine since it is portable, inexpensive and non-ionizing. However, acquisition and interpretation of ultrasound images heavily rely on the skill and expertise of the examiner, which indicates a strong need for training opportunities. An alternative to training on actual patients or volunteers is training on ultrasound simulators [1]. Ray-based simulations require an accurate detailed model of the anatomy and often lack a realistic appearance of ultrasound scattering texture. In contrast, interpolative ultrasound simulation can generate highly realistic ultrasound images [2]. This uses previously-acquired volumetric ultrasound data, i.e. *nominal volume*, from which image slices are interpolated in real-time based on the tracked position of a mock probe, while also taking into account the tissue deformation caused by such mock probe and other interacting medical tools. Note that the nominal volume can be at any deformed state, if the ultrasound probe during training will always be in contact with tissue in a similar manner (compression state) as in the acquisition, e.g. the transrectal transducer always pushes against the prostate [3]. However, if the probe might be removed off the surface, as in any abdominal examination, an uncompressed nominal anatomical mesh and corresponding nominal ultrasound volumes are then necessitated. Accordingly, any compressed state can then be simulated, starting from the first probe contact.

Pressure-compensated (*undeformed*) volumes can also be used for panoramic reconstruction of larger fields-of-view (FOV) [4], since all volumes can then be referred back to a single nominal (undeformed) anatomical state. In most cases, large FOV reconstructions are essential in order to allow for the trainee to explore clinically meaningful ranges of anatomy. Such larger FOV reconstructions are trivial, if the probe contact stays constant across acquisition, e.g. by simple rotation for a volumetric sweep as in [3]. Nevertheless, if the geometry or location of probe contact changes across acquisitions, referring back to a single unified coordinate-frame becomes essential for reconstruction. Without such compensation, not only that the internal anatomy will not align properly between separate scans, but also probe footprints in images will present an artifact along the surface during large FOV reconstruction as seen in Fig. 1.

Ultrasound imaging involves beam-forming signal intensities from the echos along rays emanating from the transducer surface. For a convex 3D probe, these rays lie in a roughly fan-shaped spherical coordinate system. For display and processing convenience, these are later sampled on a Cartesian grid; this process being called *scan-conversion*. We

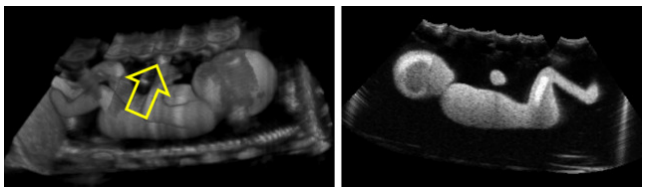

Fig. 1. Volumetric reconstruction from multiple 3D mechanically-swept scans with position tracking, where probe footprints result in unrealistic (wavy) skin appearance.

This work was supported by the Swiss Commission for Technology and Innovation (CTI).

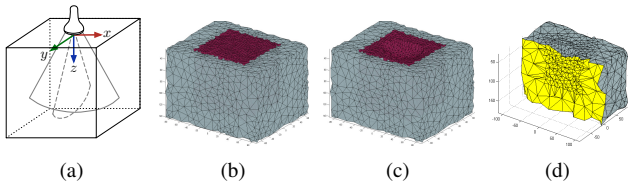

(a) (b) (c) (d)

Fig. 2. Coordinate frame in relation to the probe (a). A nominal mesh of the tissue (b) and its compressed state with the probe pressure during image acquisition (c) as well as a cross section of the mesh with compression (d).

also show in this paper that pre-scan-converted image data is required in order not to compromise image fidelity and texture realism during deformation correction.

2. METHODS

In this work, we propose a method to correct for tissue deformation caused by probe pressure during acquisitions. We employ a generic homogeneous representation of the tissue in the imaged volume, and use finite-element method (FEM) to estimate deformation caused by the known surface geometry of the probe contact area. The position and orientation of acquired volumes are recorded using an attached position tracking sensor. For undeforming each volume, the tip of the probe (the top-center of the mid-elevation image) is then assumed as the origin for the following calculations with the coordinate frame oriented as shown in Fig. 2(a).

In the proposed acquisition protocol, the transducer is held perpendicular to the skin and the probe position prior to compression when the probe is barely touching the skin surface is recorded. Afterwards, the transducer is compressed orthogonal to skin surface to acquire an image, and the compressed position is also recorded. This position is then projected on z–axis to estimate the compression magnitude δ to be used in pressure compensation. Note that due to ultrasound-gel lubrication, the forces on the body are mainly normal to skin surface, even for a tilted probe.

To undeform the volume, we use the FEM to approximate the compression over a tetrahedral mesh of the nominal state covering the imaging field-of-view. This is meshed by *iso2mesh* [5] as seen in Fig. 2(b). Finer elements are used near the superficial central region, where the probe contact occurs, in order to simulate higher-strain local deformation accurately. To simulate the deformation due to probe indentation, a model of the probe surface is used. Such a model can be obtained from the CAD design of the transducer or by 3D (e.g. laser) scanning. The scan-head of the mechanically-swept convex 3D transducer used in this work, an Analogic (Ultrasonix) 4DC7-3/40, has a roughly ellipsoid shape with an image plane radius r_1 of 40 mm and sweeping curvature r_2 of 25 mm. Accordingly, its contact surface is hereby geometrically approximated by an ellipsoid with semi-axes $a = r_1$ and $b = c = r_2$, centered at position $(x_0, y_0, z_0) = (0, 0, \delta - c)$ for a compression of δ. Then, all FEM mesh nodes on tissue surface that lies within this ellipsoid, i.e.

$$(x - x_0)^2/a^2 + (y - y_0)^2/b^2 + (z - z_0)^2/c^2 < 1,$$

are applied a displacement condition $z_d > 0$ in the z-axis to bring them onto the surface of this ellipsoid, i.e.

$$(x - x_0)^2/a^2 + (y - y_0)^2/b^2 + (z + z_d - z_0)^2/c^2 = 1\ .$$

These compressed nodes are applied zero-force constraints in the other two axes, x and y, as with the coupling gel they are free to slide along the transducer surface during compression. The depth of the meshed volume is assumed to be sufficiently large for the stresses caused by the surface compression to be negligible near the bottom surface (this is also commonly observed in abdominal imaging when the imaging depth is over 70-80 mm). Accordingly, fundamental displacement constraints in all axes are applied on the nodes at the bottom surface of the model. Given internal elasticity distribution, a stiffness matrix K is formed and the FEM problem

$$Ku = f$$

is solved with the above boundary conditions. The displacements u of all nodes then indicate the deformed state of the tissue domain as in Fig. 2(c).

The nodal displacements u and FEM basis functions together define a displacement vector field V, using which the undeformed voxel volume can be determined from the deformed acquisition by linear interpolation. Using post-scan-converted data significantly degrades the inherent ultrasound texture, as shown later in Section 3. Thus, we propose to employ the pre-scan-converted image data by incorporating the volume undeformation into scan-conversion itself. In the final undeformed image, a voxel as (x, y, z) should be assigned the intensity at $(x + V_x, y + V_y, z + V_z)$ in the deformed volume. We convert this position to the beamformed (semi-spherical) ultrasound coordinates (r,θ,ϕ) for a mechanically-swept transducer as:

$$\begin{aligned}\theta &= \text{atan2}(y + V_y, z + V_z + r_2)\\ \phi &= \text{atan2}(r_{\text{tmp}} - r_2 + r_1, x + V_x)\\ r &= \sqrt{(x + V_x)^2 + r_{\text{tmp}}^2},\end{aligned}$$

with $r_{\text{tmp}} = \sqrt{(y + V_y)^2 + (z + V_z + r_2)^2}$, and compute the intensity at that position in the pre-scan-converted data by linear interpolation.

3. RESULTS

Experiments were conducted on the CIRS fetal ultrasound biometrics (model 068) phantom shown in Fig. 1, as well as

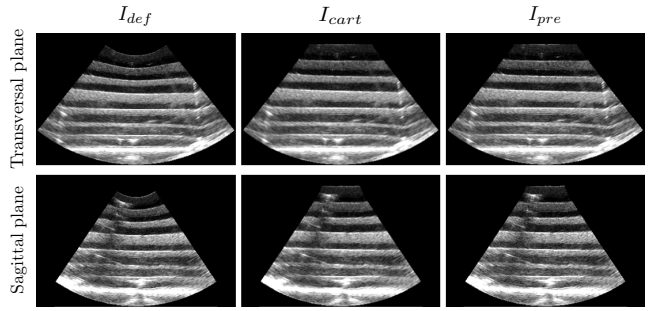

Fig. 3. Comparison of a compressed image of the layered phantom and the uncompressed volumes using Cartesian domain and the uncompression integrated into scan-conversion.

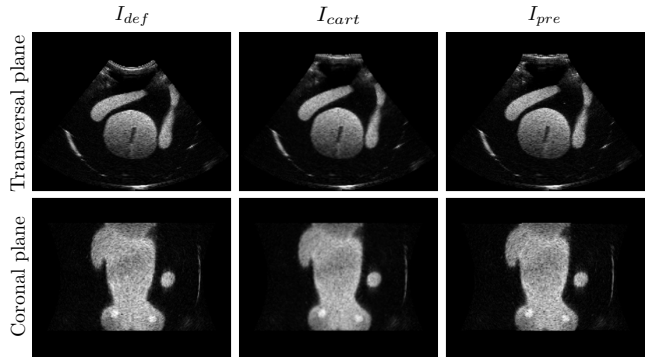

Fig. 4. Comparison of a compressed and uncompressed volumes of the fetal CIRS phantom.

a layered gelatin phantom in order to visually verify the proposed undeformation volumetrically. Alternating layers were generated using 6% and 7.5% gelatin-water concentrations, with the former having flour for scattering while the latter having no scatterers. For the stiffness matrix K of the compression model, we used linearly-elastic isotropic material assumption with a Young's modulus of 10^4 KPa. A relatively low Poisson's ratio of 0.45 was chosen considering the Zerdine/gelatin materials of these phantoms. Image acquisition was performed on an Ultrasonix SonixTouch machine with a convex 4D probe (4DC7-3/40), optically tracked using an Atracsys easyTrack500 system.

In Fig. 3, transversal and sagittal views of the gelatin phantom are seen before (I_{def}) and after compression correction of post- (I_{cart}) and pre-scan-converted (I_{pre}) image data. With the proposed correction, the flat phantom surface is seen to be recovered, in contrast to the bowl-like footprint of the probe in the original acquisitions. Fig. 4 shows similar successful surface recovery and artifact removal for the fetal phantom acquisition.

With correction using post-scan-converted data, the ultrasound texture in both volumes are observed to be smoothed, thereby degrading realism of a subsequent simulation. Integrating the compression compensation into scan-conversion process is seen to preserve the original texture. This is in particular important near the probe contact, where large strains can degrade already scan-converted data through subsequent interpolation, whereas integration into scan-conversion utilizes the denser pre-scan-converted data closer to the probe. Table 1 shows this quantitatively through the standard deviation σ of B-mode intensity variation in different homogeneous image regions, i.e. the top and bottom of the gelatin phantom and in the abdominal area of the fetal phantom. From σ normalized to the baseline value, it is seen that integration of correction into scan-conversion has merely 1% worst-case variation loss in contrast to a 35% loss when pressure compensating posterior to scan-conversion. Additionally, the histograms of these homogeneous regions are compared by computing the χ^2 distance. The histograms of deformation integrated into scan-conversion match the histogram of the original image up to 90% better compared to that of post-scan-conversion compensation.

Table 1. Comparison of changes in ultrasound texture by undeforming images

	I_{def}	I_{cart}	I_{pre}	$I_{\text{def}} - I_{\text{cart}}$	$I_{\text{def}} - I_{\text{pre}}$
σ_{top}	7.9	5.1	7.8	35%	1%
σ_{bottom}	12.2	9.9	12.3	19%	1%
σ_{fetus}	16.5	14.8	16.7	10%	1%
χ^2_{top}	0	259	21		
χ^2_{bottom}	0	1815	904		
χ^2_{fetus}	0	215	61		

The proposed method can correct for a high level of probe pressure as shown in Fig. 5. The original images I_{def} along with the pressure corrected images I_{pre} are shown. For each level of compression we get parallel layers as demonstrated by the edge images. While the edges are curved in the compressed images especially near the probe they are flat after pressure correction. Thus we also verified that the homogeneity assumption holds. Although the phantom was made of layers with different amounts of gelatin all layers, the stiff as well as the limp ones, are correctly undeformed.

Fig. 6 shows pressure corrected images stitched to an extended FOV volume, where the "wavy" surface artifact is eliminated through our proposed correction.

Computations with our non-optimized Matlab implementation took 5 min on an Intel i7-4770K processor for a mesh with 14000 nodes and a volume with $350 \times 280 \times 290$ voxels; in addition to a one-time 15 min computation of the stiffness matrix. Note that several deformations can be precomputed to allow for rapid pressure compensation. Also, given a linear FEM approximation the deformation scales linearly for linearly changing constraints, which can be utilized to accelerate the correction process. Reference displacements u_{ref} from a unit compression or a maximum potential compression magnitude δ_{ref} can be used to approximate other deformations $u = u_{\text{ref}} \cdot \delta / \delta_{\text{ref}}$.

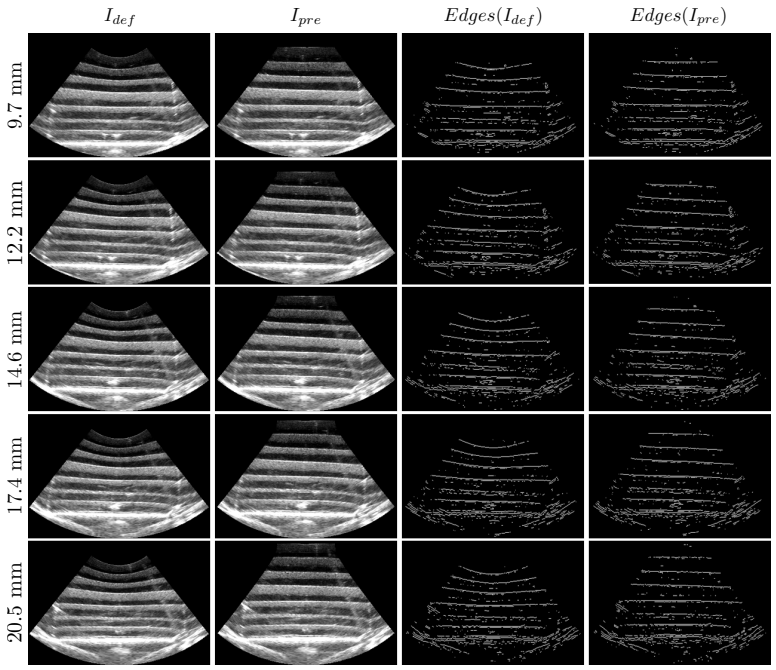

Fig. 5. Deformed and pressure corrected images for different compression magnitudes as well as edges detection results in the axial direction to show the recovery of flat interfaces.

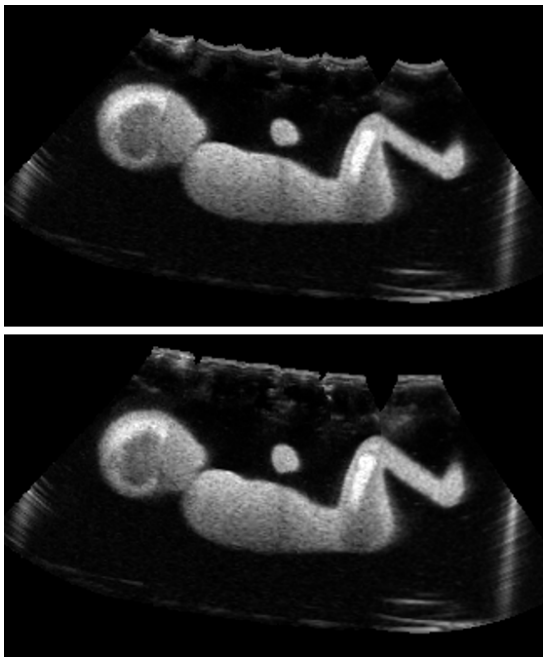

Fig. 6. Comparison of extended volume based on compressed volumes and undeformed volumes.

4. DISCUSSION AND CONCLUSIONS

We proposed a method to correct for probe pressure in the acquired ultrasound volumes to be used in image-based ultrasound simulation. Using our approach, the artifacts of probe footprints are eliminated from the volumes, enabling the fusion of several individual acquisitions into a large field-of-view reconstruction. Thanks to the integration of the correction into the scan-conversion process, the ultrasound texture fidelity could be maintained during pressure compensation.

We hereby chose a box-shaped representation with a *flat* top surface. This was inline with the surface geometry of the phantoms used. Note that the surface geometry is mostly relevant under the relatively small area of probe contact, since due to the fan shaped image field-of-view, no imaging data exists close to the surface outside the probe footprint. For in-vivo acquisitions, one can use a semi-spherical or more complex surface models. This will allow for a convex surface appearance, instead of flat, when several volumes are fused. Additionally, instead of an undeformed state, all compensation could also target any given reference state that may potentially also be deformed, e.g. under gravity. Pressure compensation and subsequent volumetric reconstruction from in-vivo acquisitions will be studied next.

Although the internal geometry and elasticity distribution of tissue can be estimated using, for instance, elastography [6], we hereby used a generic homogeneous representation of the tissue for the purposes of compression correction. This is found to be sufficient in most cases since the skin surface is devoid of strong boundary effects such as bones. Additionally, for training simulation use, simplicity of acquisition can be traded of with accuracy of deformation.

5. REFERENCES

[1] H. Maul, et al., "Ultrasound simulators: experience with the SonoTrainer and comparative review of other training systems," *Ultrasound Obstet Gynecol* 24(5): 581–585, 2004.

[2] O. Goksel and S.E. Salcudean, "B–mode ultrasound image simulation in deformable 3–D medium," *IEEE Trans Med Imaging* 28(11): 1657–1669, 2009.

[3] O. Goksel, et al., "Prostate brachytherapy training with simulated ultrasound and fluoroscopy images," *IEEE Trans Biomed Eng* 60(4): 1002–1012, 2013.

[4] T. Poon and R. Rohling, "Three–dimensional extended field–of–view ultrasound," *Ultras Med Biol* 32(3): 357–369, 2006.

[5] Q. Fang and D.A. Boas, "Tetrahedral mesh generation from volumetric binary and gray–scale images," *Proceedings ISBI 2009*: 1142–1145, 2009.

[6] J. Gennisson, et al., "Ultrasound elastography: principles and techniques," *Diagn Interv Imaging* 94(5): 487–95, 2013.